Injection molded polymeric hard X-ray lenses

Stöhr, Frederik; Simons, Hugh; Jakobsen, Anders Clemen; Nielsen, Claus Højgård; Michael-Lindhard, Jonas; Jensen, Flemming; Poulsen, Henning Friis; Hansen, Ole; Hübner, Jörg

Published in:
Optical Materials Express

Link to article, DOI:
10.1364/OME.5.002804

Publication date:
2015

Document Version
Publisher's PDF, also known as Version of record

Injection molded polymeric hard X-ray lenses

F. Stöhr,[1,*] H. Simons,[2] A. C. Jakobsen,[2] C. H. Nielsen,[1] J. Michael-Lindhard,[1] F. Jensen,[1] H. F. Poulsen,[2] O. Hansen[3] and J. Hübner[1]

[1]DTU Danchip, Technical University of Denmark, Kgs. Lyngby DK-2800, Denmark
[2]Department of Physics, Technical University of Denmark, Kgs. Lyngby DK-2800, Denmark
[3]DTU Nanotech and CINF, Technical University of Denmark, Kgs. Lyngby DK-2800, Denmark
[*]frsto@danchip.dtu.dk

Abstract: A novel and economical approach for fabricating compound refractive lenses for the purpose of focusing hard X-rays is described. A silicon master was manufactured by UV-lithography and deep reactive ion etching (DRIE). Sacrificial structures were utilized, which enabled accurate control of the etching profile and were removed after DRIE. By electroplating, an inverse nickel sample was obtained, which was used as a mold insert in a commercial polymer injection molding machine. A prototype lens made of polyethylene with a focal length of 350 mm was tested using synchrotron radiation at photon energies of 17 keV. A 55 µm long line focus with a minimal waist of 770 nm (FWHM) and a total lens transmittance of 32% were measured. Due to its suitability for cheap mass production, this highly efficient optics may find widespread use in hard X-ray instruments.

OCIS codes: (340.0340) X-ray optics; (340.6720) Synchrotron radiation; (340.7460) X-ray microscopy; (080.2205) Fabrication, injection molding; (220.4000) Microstructure fabrication; (220.3630) Lenses

References and links

1. G. E. Ice, J. D. Budai, and J. W. L. Pang, "The race to x-ray microbeam and nanobeam science," Science **334**(6060), 1234–1239 (2011).
2. H. Simons, A. King, W. Ludwig, C. Detlefs, W. Pantleon, S. Schmidt, I. Snigireva, A. Snigirev, H. F. Poulsen, and H. F. Poulsen, "Dark-field X-ray microscopy for multiscale structural characterization," Nat. Commun. **6**, 6098 (2015).
3. A. Snigirev, V. Kohn, I. Snigireva, and B. Lengeler, "A compound refractive lens for focusing high-energy X-rays," Nature **384**(6604), 49–51 (1996).
4. B. Lengeler, C. G. Schroer, B. Benner, T. F. Günzler, M. Kuhlmann, J. Tümmler, A. S. Simionovici, M. Drakopoulos, A. Snigirev, and I. Snigireva, "Parabolic refractive X-ray lenses: a breakthrough in X-ray optics," Nucl. Instruments Methods Phys. Res. Sect. A **467–468**, 944–950 (2001).
5. V. V. Aristov, M. V. Grigoriev, S. M. Kuznetsov, L. G. Shabelnikov, V. A. Yunkin, M. Hoffmann, and E. Voges, "X-ray focusing by planar parabolic refractive lenses made of silicon," Opt. Commun. **177**(1-6), 33–38 (2000).
6. B. Wu, A. Kumar, and S. Pamarthy, "High aspect ratio silicon etch: A review," J. Appl. Phys. **108**(5), 051101 (2010).
7. F. Stöhr, J. Wright, H. Simons, J. Michael-Lindhard, J. Hübner, F. Jensen, O. Hansen, and H. F. Poulsen, "Optimizing shape uniformity and increasing structure heights of deep reactive ion etched silicon X-ray lenses," J. Micromech. Microeng. **25**(12), 125013 (2015).
8. C. G. Schroer, O. Kurapova, J. Patommel, P. Boye, J. Feldkamp, B. Lengeler, M. Burghammer, C. Riekel, L. Vincze, A. van der Hart, and M. Küchler, "Hard x-ray nanoprobe based on refractive x-ray lenses," Appl. Phys. Lett. **87**(12), 124103 (2005).
9. A. F. Isakovic, A. Stein, J. B. Warren, S. Narayanan, M. Sprung, A. R. Sandy, and K. Evans-Lutterodt, "Diamond kinoform hard X-ray refractive lenses: design, nanofabrication and testing," J. Synchrotron Radiat. **16**(Pt 1), 8–13 (2009).
10. L. Alianelli, K. J. S. Sawhney, A. Malik, O. J. L. Fox, P. W. May, R. Stevens, I. M. Loader, and M. C. Wilson, "A planar refractive x-ray lens made of nanocrystalline diamond," J. Appl. Phys. **108**(12), 123107 (2010).
11. M. Polikarpov, I. Snigireva, J. Morse, V. Yunkin, S. Kuznetsov, and A. Snigirev, "Large-acceptance diamond planar refractive lenses manufactured by laser cutting," J. Synchrotron Radiat. **22**(Pt 1), 23–28 (2015).
12. A. Q. R. Baron, Y. Kohmura, Y. Ohishi, and T. Ishikawa, "A refractive collimator for synchrotron radiation," Appl. Phys. Lett. **74**(10), 1492–1494 (1999).
13. J. T. Cremer, M. A. Piestrup, H. R. Beguiristain, C. K. Gary, R. H. Pantell, and R. Tatchyn, "Cylindrical compound refractive x-ray lenses using plastic substrates," Rev. Sci. Instrum. **70**(9), 3545–3548 (1999).

#249271 Received 2 Sep 2015; revised 31 Oct 2015; accepted 5 Nov 2015; published 11 Nov 2015

14. M. Piestrup, J. T. Cremer, H. R. Beguiristain, C. K. Gary, and R. H. Pantell, "Two-dimensional x-ray focusing from compound lenses made of plastic," Rev. Sci. Instrum. **71**(12), 4375 (2000).
15. V. Nazmov, E. Reznikova, J. Mohr, A. Snigirev, I. Snigireva, S. Achenbach, and V. Saile, "Fabrication and preliminary testing of X-ray lenses in thick SU-8 resist layers," Microsyst. Technol. **10**(10), 716–721 (2004).
16. F. Pérennès, M. Matteucci, W. Jark, and B. Marmiroli, "Fabrication of refractive X-ray focusing lenses by deep X-ray lithography," Microelectron. Eng. **78–79**, 79–87 (2005).
17. V. Nazmov, J. Mohr, I. Greving, M. Ogurreck, and F. Wilde, "Modified x-ray polymer refractive cross lens with adiabatic contraction and its realization," J. Micromech. Microeng. **25**(5), 055010 (2015).
18. B. Cederström, M. Lundqvist, and C. Ribbing, "Multi-prism x-ray lens," Appl. Phys. Lett. **81**(8), 1399 (2002).
19. M. Simon, E. Reznikova, V. Nazmov, T. Grund, A. Last, M. Denecke, and C. T. Walker, "A new type of X-ray condenser lenses with large apertures fabricated by rolling of structured films," AIP Conf. Proc. **1221**, 85–90 (2010).
20. P. Nillius, S. Karlsson, B. Cederström, E. Fredenberg, and M. Danielsson, "Large-aperture focusing of high-energy x rays with a rolled polyimide film," Opt. Lett. **36**(4), 555–557 (2011).
21. W. Jark, "On aberrations in saw-tooth refractive X-ray lenses and on their removal," J. Synchrotron Radiat. **18**(2), 198–211 (2011).
22. G. Pavlov, I. Snigireva, A. Snigirev, T. Sagdullin, and M. Schmidt, "Refractive X-ray shape memory polymer 3D lenses with axial symmetry," XRay Spectrom. **41**(5), 313–315 (2012).
23. F. Stöhr, J. Michael-Lindhard, J. Hübner, F. Jensen, H. Simons, A. C. Jakobsen, H. F. Poulsen, and O. Hansen, "Sacrificial structures for deep reactive ion etching of high-aspect ratio kinoform silicon X-ray lenses," J. Vac. Sci. Technol. B **33**(6), 062001 (2015).
24. F. Stöhr, J. Michael-lindhard, H. Simons, H. F. Poulsen, J. Hübner, O. Hansen, J. Garnaes, and F. Jensen, "Three-dimensional nanometrology of microstructures by replica molding and large-range atomic force microscopy," Microelectron. Eng. **141**, 6–11 (2015).
25. M. Matschuk and N. B. Larsen, "Injection molding of high aspect ratio sub-100 nm nanostructures," J. Micromech. Microeng. **23**(2), 025003 (2013).
26. B. Kobrin, J. Chinn, R. Nowak, and R. Yi, "Functional organic based vapor deposited coatings adhered by an oxide layer," US Patent Application 2007/0020392 A1 (2007).
27. J. Cech and R. Taboryski, "Stability of FDTS monolayer coating on aluminum injection molding tools," Appl. Surf. Sci. **259**, 538–541 (2012).
28. R. K. Kupka, F. Bouamrane, C. Cremers, and S. Megtert, "Microfabrication: LIGA-X and applications," Appl. Surf. Sci. **164**(1-4), 97–110 (2000).
29. V. Nazmov, E. Reznikova, J. Mohr, V. Saile, L. Vincze, B. Vekemans, S. Bohic, and A. Somogyi, "Parabolic crossed planar polymeric x-ray lenses," J. Micromech. Microeng. **21**(1), 015020 (2011).

1. Introduction

Refractive X-ray lenses are versatile optical components in synchrotron beamlines and act e.g. as condensers or objectives in hard X-ray microscopes [1,2]. They are characterized by their low refractive power, necessitating radii of curvature (R) in the lower micrometer range and the combination of many such lenses in a compound refractive lens (CRL) in order to achieve practical focal lengths [3–5].

The size and intensity gain of a focused X-ray beam shaped by a CRL comprising N concave bi-parabolic lenslets are limited by photon absorption and Compton scattering [4]. For a given lens with focal length f, refractive index n and attenuation coefficient μ, a material specific absorption limited aperture D_{eff} can be calculated by the $1/e^2$ width of the intensity transmission profile well approximated by:

$$D_{\mathrm{eff}} = \sqrt{\frac{8R}{\mu N}} = \sqrt{\frac{16 f (1-n)}{\mu}}. \qquad (1)$$

Figure 1 shows D_{eff} for various lens materials as a function of X-ray energy (E) at a fixed focal length of ~300 mm (a typical value). The superior transmittance of beryllium with an atomic number $Z = 4$ justifies its frequent use at synchrotron radiation facilities [4]. However, its manufacture by embossing is a) a serial process that necessitates high precision assembly of single lenslets, and b) practically limits R to ≥ 50 μm, requiring long lenses and limiting achievable focal lengths.

In the case of silicon, its inferior optical properties are outweighed by advanced structuring techniques such as deep reactive ion etching [6,7]. Multiple planar CRLs were precisely fabricated on a single silicon wafer, allowing X-ray focusing down to a spot size of ~50 nm [8]. Different attempts were undertaken to exploit the unique material properties of

#249271 Received 2 Sep 2015; revised 31 Oct 2015; accepted 5 Nov 2015; published 11 Nov 2015

diamond, but their success has typically been hindered by the high cost of single crystals, the shallowness of the lens structures [9,10] or rough-textured lens surfaces [11].

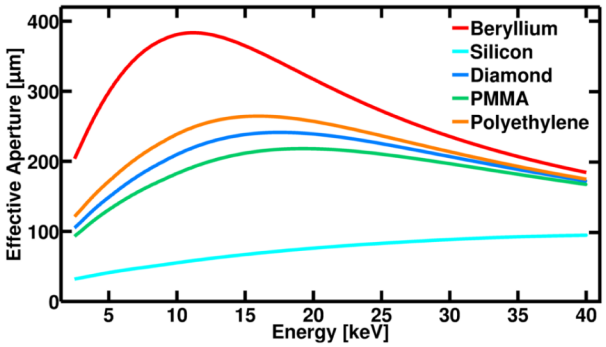

Fig. 1. Material specific effective apertures of lenses with focal lengths of 300 mm as a function of X-ray energy.

Polymers composed primarily of hydrogen, oxygen and carbon show similar transmittance to diamond, and have subsequently been used for X-ray lenses [12–14]. While lenses made of PMMA and epoxy-based SU-8 are routinely used in synchrotron beamlines [15–17], their common manufacture by rarely available X-ray lithography is expensive. As an economic alternative, polymeric multi-prism lenses were molded from anisotropically etched silicon masters [18,19] or structured by laser ablation [20]. However, these optics face technological challenges when sub-micron focusing is required [21]. A photopolymer was used to obtain rotationally symmetric lenses [22], but individual lenslets were produced serially, resulting in long production times and similar issues as with embossing beryllium.

In this article we propose a novel route for X-ray lens manufacture that harnesses the high transmittance of low-Z thermoplastics and is suitable for cheap mass production, while capitalizing on the technological advantages of structuring silicon without sacrificing achievable resolution. CRLs made of polyethylene (PE) were injection molded from a nickel mold insert produced by electroforming from an etched silicon master. Compared to silicon, PE has a fourfold greater D_{eff} at 15 keV (Fig. 1), enabling one to halve the achievable spot size with a tenfold increase in photon flux density (i.e. gain) considering a line-focusing lens.

2. Micro fabrication

The lenses were developed at DTU Danchip, the microfabrication facility at the Technical University of Denmark (Fig. 2). The target features were arrays of bi-parabolic cylindrical cavities with R = 50 µm, lateral dimensions of 450 µm × 300 µm and depths of 200 µm. The manufacture of the silicon master included standard UV-lithography and pattern transfer by reactive ion etching into a thermally grown 700 nm thick silicon oxide layer, which served as a hard mask for DRIE of the silicon using an optimized Bosch process (Pegasus, SPTS).

#249271 Received 2 Sep 2015; revised 31 Oct 2015; accepted 5 Nov 2015; published 11 Nov 2015

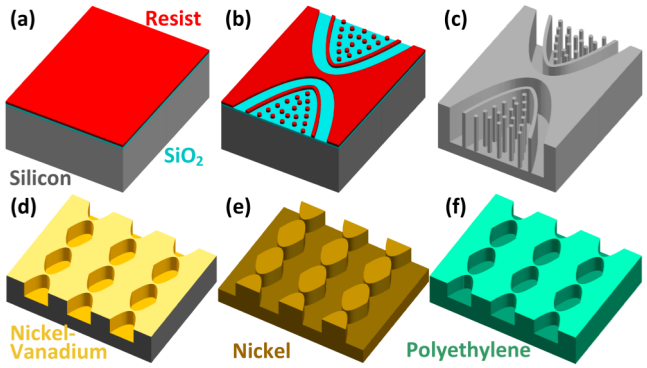

Fig. 2. Process flow for injection molded X-ray lenses. (a) The starting material is a 4-inch Si wafer covered with SiO_2 and photo resist. (b) The resist and SiO_2 are patterned by UV-lithography and reactive ion etching, respectively. (c) Deep reactive ion etching of silicon. (d) Removal of sacrificial structures and deposition of a metal seed layer. (e) Nickel electroplating and silicon removal. (f) Polymer injection molding in polyethylene.

DRIE was a critical process step in ensuring the near-90° sidewalls required to guarantee both lens uniformity and the successful release of the polymeric part from the mold. To this end, we utilized sacrificial structures, which facilitated accurate profile control [23]. Figures 3(a) and 3(b) illustrate these structures, where a 15 µm wide trench defines the perimeter of a silicon cavity, a thin wall confines the trench and the remaining space inside the cavities was uniformly filled with pillars. This design reduced the etch load and allowed a local control of the etch depth by adapting the mean spacing between pillars to the width of the trench. The thickness of the wall was 4 µm and the diameter of the pillars 5 µm, which allowed their complete thermal oxidation after DRIE and their selective removal by etching in hydrofluoric acid (Figs. 3(c) and 3(d)).

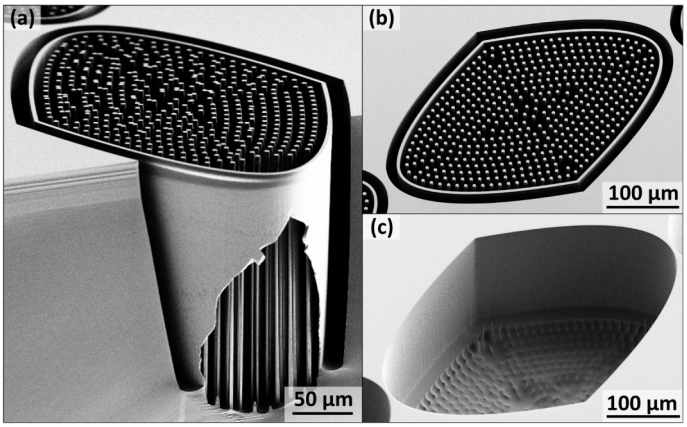

Fig. 3. Scanning electron micrographs of the silicon master. (a), (b) Cross sections illustrating the sacrificial structures. (c), (d) Top views of cavities before and after the removal of sacrificial structures.

Optical profilometry confirmed that the etched sidewalls were slightly positively tapered by 0.5°, which favored a successful release of the injection molded polymeric part. The parabolic shape at the apex of the silicon cavities was characterized based on atomic force microscopy [24]. Due to the slightly tapered sidewall, R varied by ± 2% along the 200 µm deep structure. We accepted this minor deviation from an ideal cylindrically parabolic shape for the first demonstration of the injection molded polymeric lenses.

To obtain the mold insert, the silicon master was first uniformly covered with a 70 nm thick layer of amorphous silicon by low pressure chemical vapor deposition (LPCVD), sputter

#249271 Received 2 Sep 2015; revised 31 Oct 2015; accepted 5 Nov 2015; published 11 Nov 2015

coated with a 50 nm thick seed layer of a nickel-vanadium alloy, and then conformably electroplated with nickel (microform.200, Technotrans). By dissolving the silicon in aqueous potassium hydroxide (KOH), a 550 µm thick nickel wafer was obtained, which included the inverse lens structures (Figs. 4(a) and 4(b)). The nickel surface was functionalized with a self-assembled monolayer of a fluorocarbon-containing thin film (FDTS) using molecular vapor deposition (MVD) [25]. A shim was cut from the wafer by laser micro machining and inserted into the tool of an ENGEL Victory Tech injection molding machine.

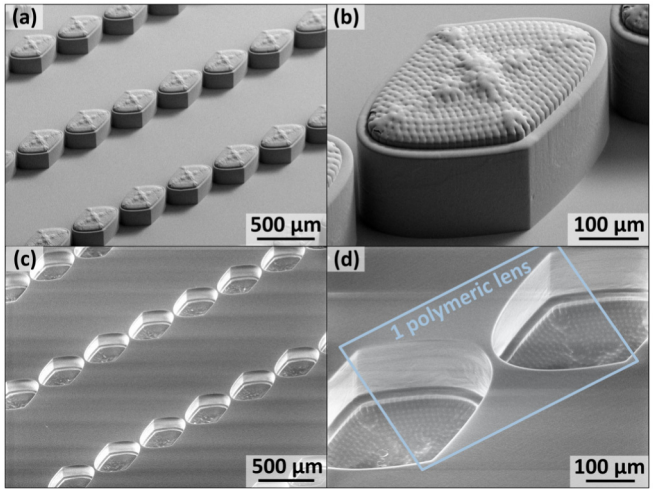

Fig. 4. Scanning electron micrographs of the nickel mold insert (a), (b) and of the injection molded polymeric lenses (c), (d).

3. Polymer injection molding

Linear low-density polyethylene (LLDPE, Flexirene® MT40A, Versalis) was used as the thermoplastic, due to its high melt flow rate, flexibility and high shrinkage upon solidification, which in combination guaranteed uniform mold filling and eased the release of the polymeric part. LLDPE is characterized by a low degree of crystallinity, which reduces small angle X-ray scattering at grain boundaries. Its chemical formula is $(C_2H_4)_n$ and its density as specified by our supplier is 0.925 g/cm^3 (μ = 0.523 cm^{-1}, refractive index decrement $\delta = (1 - n) = 7.584 \times 10^{-07}$ for E = 17 keV).

Polymeric chips with dimensions of 1 × 26 × 76 mm^3 comprising 20 CRLs with up to N = 143 lenslets each and additional trenches for alignment were injection molded. A variotherm process with a cycle time of ~5 min was optimized. The nozzle temperature was 200°C, the injection speed 50 cm^3/s, the injection and holding pressures 600 bar, and the holding time 10 s. The mold temperature was 100°C during polymer injection (i.e. above the glass transition temperature of LLDPE) and was cooled below 25°C for releasing the polymeric part.

Figures 4(c) and 4(d) show the final injection molded X-ray lenses. The lens sidewalls do not reveal any notable difference to the silicon master. The lens top surface was inspected by optical microscopy and the geometrical shape was analyzed by fitting parabolas to the lens edges, resulting in R = 52.5 ± 0.5 µm and a mean deviation from a perfect parabola of ~700 nm (Fig. 5). The deviation from the nominal shape is due to polymer shrinking, which needs to be compensated for in future. Buckling of the parabola apex is visible, which is more pronounced on the right parabola and indicates local mechanical stress.

#249271 Received 2 Sep 2015; revised 31 Oct 2015; accepted 5 Nov 2015; published 11 Nov 2015

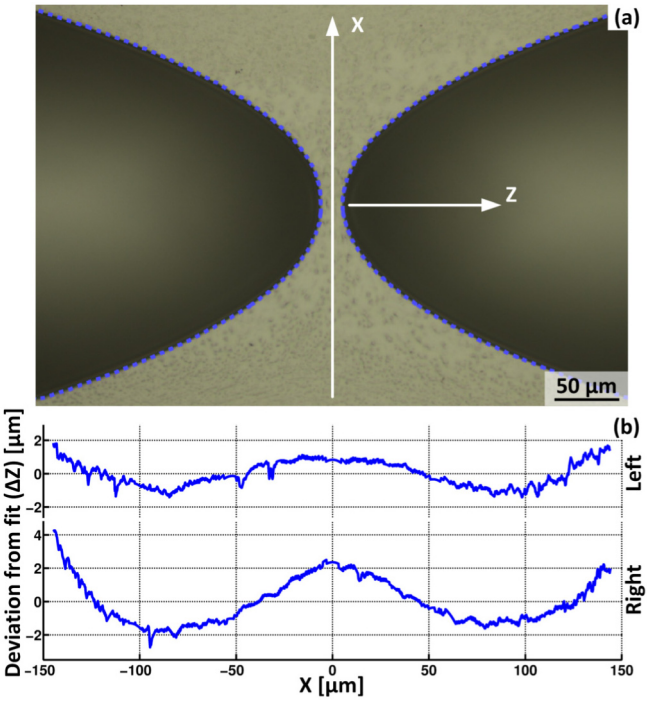

Fig. 5. (a) Image of the top surface of a polymeric lenslet. The detected edge is highlighted by a dashed line. (b) Differences between the detected edges and the fit curves of the left and right parabolas.

The most critical step during injection molding was the release of the polymeric part from the mold, which, if non-optimal, mostly affected the bridges between individual lens cavities. Figures 6(a) and 6(b) show these regions of lens structures with bridge thicknesses d = 20 µm and d = 5 µm, respectively. While the 20 µm thick bridge is mostly intact, deformations and partial rupture of the 5 µm thick bridge are clearly visible. This indicates that the latter bridge caused sticking of the polymeric part on the nickel mold and the part was released under mechanical stress. Since we included both structures on the same mold next to each other, mechanical strain on one feature also affected the other. Hence, a future iteration needs to guarantee a release free of mechanical stress and a mold without any structures that may cause mechanical adhesion.

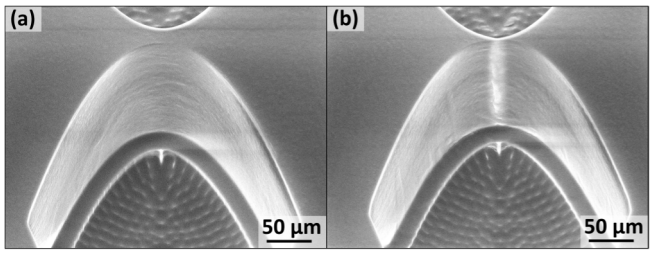

Fig. 6. Scanning electron micrographs of the bridges between polymeric lens cavities. (a) Bridge thickness d = 20 µm. (b) d = 5 µm.

4. Optical performance

The X-ray optical performance of a LLDPE CRL with R = 50 µm and N = 101 was tested by directly imaging the focused beam using a bright field X-ray microscope at the beamline ID06

#249271 Received 2 Sep 2015; revised 31 Oct 2015; accepted 5 Nov 2015; published 11 Nov 2015

at the European Synchrotron Radiation Facility (ESRF) illustrated in Fig. 7(a). The polymeric lens was mounted for vertical focusing 51 m downstream the undulator source and the X-ray energy was set to E = 17 keV by a Si(111) double monochromator ($\Delta E/E = 1.4 \times 10^{-4}$). A second CRL composed of 71 beryllium lenslets with R = 50 µm and a focal length p = 0.325 m was used as an X-ray objective to image the focused beam at a distance q = 4.71 m, giving a magnification $M_{\text{X-ray}} = q/p = 14.5$. A high-resolution detector comprising a scintillator screen coupled by microscope optics with magnification M_{Vis} = 10 to a FreLoN CCD camera with pixelsize Res_{CCD} = 14 µm was used. This yields a theoretical spatial resolution of $Res_{\text{CCD}}/M_{\text{Vis}}/M_{\text{X-ray}}$ = 97 nm.

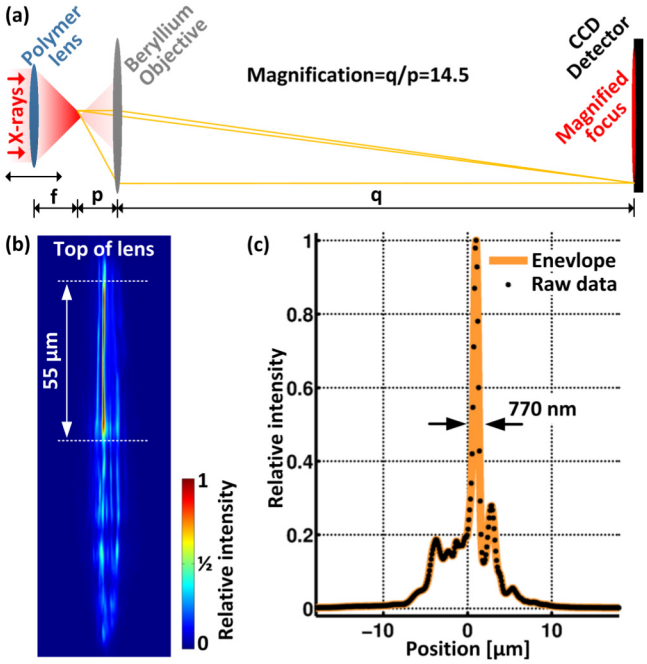

Fig. 7. (a) Setup for optical tests. (b) Image of the focal line at f = 348 mm (see Visualization 1). (c) Summed intensity of the 55 µm long section marked in (b).

Beam profiles were recorded while the position of the objective was fixed and the polymeric lens moved along the optical axis (see Visualization 1). A 55 µm-long line focus with a full width at half maximum (FWHM) of 770 nm was observed at f = 348 mm, which shows the high potential of injection molded polymeric lenses (Figs. 7(b) and 7(c)). However, the beam profile was highly irregular, whereas the uppermost part of the lens generally outperformed the lowermost. The complete, 140 µm-long line was 2.7 µm wide (FWHM) at f = 325 mm. The total transmittance of the lens was 32%, which corresponds to a gain in photon flux density of 125, assuming the measured 770 nm small focus and neglecting the large tails around the peak. For an ideal lens a transmittance of ~50%, a spot size of 170 nm and a gain of 600 were expected.

5. Discussion

This first optical test demonstrated the potential of injection molded X-ray lenses and future improvements can be readily realized. The observed irregularities in the beam profile likely originated from mechanical deformations of the lenses that occurred during the release of the polymeric part in the injection molding process. We anticipate that avoiding mechanical stress during demolding would substantially improve the optical performance of the lenses. The mold insert could be redesigned, such that friction is largely reduced, or additional ejector pins could be integrated into the tool to result in a more gentle release. The deposition of a

#249271 Received 2 Sep 2015; revised 31 Oct 2015; accepted 5 Nov 2015; published 11 Nov 2015

thin layer of SiO_2 or Al_2O_3 by atomic layer deposition onto the nickel sample prior to MVD may increase the surface coverage and promote the adhesion of the anti-stiction coating applied [26]. Using thermoplastics with higher shrinking coefficients may further reduce mechanical adhesion.

The discrepancy in photon transmittance was partially due to a slight warpage of the polymeric chip, which reduced the effective depth of the lens from 200 μm to 140 μm. Furthermore, our polymer maybe contained residues of high-*Z* atomic species, which caused additional X-ray absorption.

The height of the lenses can be increased by optimizing DRIE during fabrication of the silicon master, which may include a redesign of sacrificial structures to guarantee deeper vertical etching. The encountered variation of the radius of curvature along the height of the lenses $\Delta R = \pm 2\%$ directly relates to a variation in focal length via $\Delta f = \Delta R / 2N\delta = \pm 2\%$. This variation must be reduced in the future, since it is significantly larger than the depth of focus (~1 mm [7]). A more accurate control of the sidewall profile can readily be achieved by means of a more extensive optimization of the etching process of the silicon master [23]. Although, in terms of economy, this will consume additional resources, it will be insignificant, not least because we expect that more than 1000 polymeric parts may be obtained from a single master [27]. As an alternative to DRIE of silicon, X-ray lithography may be used to produce the mold insert [28].

We have no evidence for the degradation of the polymer in the X-ray beam over the course of the ~10 h long experiments. Comparable lenses made of SU-8 by X-ray lithography routinely produce focused X-ray beams with sub-micron spot sizes (FWHM) which are stable over extended time periods [29]. Restricting the use of polymeric lenses to shaping weak X-ray beams such as strongly monochromatized synchrotron radiation as in our study or those generated by X-ray tubes in small laboratory instruments would relax the requirement on radiation stability. However, long-term tests remain necessary to verify the radiation stability of the lenses made of PE. Polystyrene (PS) with pendant aromatic groups may be a viable alternative thermoplastic with respect to radiation resistance. Notably, however, PS is harder to process due to its generally low shrinkage and high rigidity.

6. Conclusion

Polymer injection molded lenses have proven to be promising highly efficient X-ray optics. A 55 μm long line focus with a minimal waist of 770 nm and a total lens transmittance of 32% were obtained. The proposed manufacturing route including fully automated injection molding allowed to produce lens chips comprising multiple CRLs with a final production rate of >10 pieces per hour. This indicates the economic value of injection molded X-ray lenses, which may have applications not only at synchrotron radiation facilities, but also in more readily available small laboratory X-ray instruments.

Acknowledgments

H.F. Poulsen acknowledges an ERC Advanced grant, d-TXM. O. Hansen acknowledges support from The Danish National Research Foundation's Center for Individual Nanoparticle Functionality, CINF (DNRF54). H. Simons acknowledges support from a DFF-FTP individual postdoc grant. We thank the ESRF for providing the X-ray beam and Carsten Detlefs for assistance at the beam line.

#249271 Received 2 Sep 2015; revised 31 Oct 2015; accepted 5 Nov 2015; published 11 Nov 2015